Exact Double Counting in Combining the Dynamical Mean Field Theory and the Density Functional Theory

Kristjan Haule

Phys. Rev. Lett. **115**, 196403 — Published 5 November 2015

DOI: 10.1103/PhysRevLett.115.196403

Exact double-counting in combining the Dynamical Mean Field Theory and the Density Functional Theory

Kristjan Haule
Department of Physics and Astronomy, Rutgers University, Piscataway, USA
(Dated: October 5, 2015)

We propose a continuum representation of the Dynamical Mean Field Theory, in which we were able to derive an exact overlap between the Dynamical Mean Field Theory and band structure methods, such as the Density Functional Theory. The implementation of this exact double-counting shows improved agreement between theory and experiment in several correlated solids, such as the transition metal oxides and lanthanides. Previously introduced nominal double-counting is in much better agreement with the exact double-counting than most widely used fully localized limit formula.

PACS numbers: 71.27.+a,71.30.+h

Understanding the electronic structure of materials with strong electronic correlations remains one of the great challenges of modern condensed matter physics. The first step towards calculating the electronic structure of solids has been achieved by obtaining the single-particle band dispersion $E(\mathbf{k})$ within the density functional theory (DFT) in the local density approximation (LDA) [1], which takes into account correlation effects only in a limited extent.

To account for the many-body correlation effects beyond LDA, more sophisticated methods have been developed. Among them, one of the most successful schemes is the dynamical mean-field theory (DMFT) [2]. It replaces the problem of describing correlation effects in a periodic lattice by a strongly interacting impurity, coupled to a self-consistent bath [3]. This method was first developed to solve the Hubbard model, but it was soon realized [4] that it can also be combined with the LDA method, to give more material specific predictions of correlation effects in solids. The LDA+DMFT method achieved great success in the past two decades, as it was successfully applied to numerous correlated solids [5]. The combination of the two methods, nevertheless lead to a problem of somewhat ambiguous way of subtracting the part of correlations, which are accounted for by both methods.

The so-called double-counting (DC) term was usually approximated by the formula first developed in the context of LDA+U, and was evaluated by taking the atomic limit for the Hubbard interaction term [6, 7]. Many other similar schemes were proposed recently [8–12], but rigorous derivation of this double-counted interaction in solids within DMFT and LDA is missing to date. Here we propose a new method of calculating the overlap between DMFT and a band-structure method in solids, and we explicitly evaluate this DC functional within LDA+DMFT. Some ideas presented here come from studying the toy model of correlations, namely the H_2 molecule, in which the exact double-counting was found for the DMFT method applied to the single H atom of H_2 molecule [13], where the screening is absent. The derivation of the double-counting in the presence of screening in solids will be addressed in this letter, and will be tested on several well studied correlated materials, such as transition metal oxides $SrVO_3$, $LaVO_3$, and most studied lanthanide metal, the elemental Cerium.

To compare different approximations in the same language, it is useful to cast them into the form of the Luttinger Ward functional [5, 15, 16], which is a functional of the electron Green's function G, and takes the form $\Gamma[G] = -\mathrm{Tr}((G_0^{-1} - G^{-1})G) + \mathrm{Tr}\log(-G) + \Phi_{V_c}[G]$. The first part is the material dependent part, in which $G_0^{-1}(\mathbf{r}\mathbf{r}';\omega) = [\omega + \mu + \nabla^2 - V_{ext}(\mathbf{r})]\delta(\mathbf{r} - \mathbf{r}')$, and the second two terms are universal functionals of the Green's function $G(\mathbf{r}\tau, \mathbf{r}'\tau')$ and the Coulomb interaction $V_c(\mathbf{r} - \mathbf{r}')$. In the exact theory, $\Phi_{V_c}[G]$ contains all skeleton Feynman diagram, constructed by G and V_c [16]. In the language of the Luttinger Ward functional, different approximations can then be looked at as different approximations to the interacting part $\Phi_{V_c}[G]$.

The Density Functional Theory equations can be obtained by approximating the exact functional $\Phi_{V_c}[G]$ by $E_H[\rho(\mathbf{r})] + E_{xc}[\rho(\mathbf{r})]$, where E_H and E_{xc} are the Hartree and the exchange-correlation functionals, respectively. The stationarity condition gives the DFT equations, i.e., $G^{-1} - G_0^{-1} = (V_H[\rho] + V_{xc}[\rho])\delta(\mathbf{r} - \mathbf{r}')\delta(\tau - \tau')$, because $\delta E_{xc}[\rho]/\delta G = \delta(\mathbf{r} - \mathbf{r}')\delta(\tau - \tau')$ $\delta E_{xc}[\rho]/\delta\rho = \delta(\mathbf{r} - \mathbf{r}')\delta(\tau - \tau')$ $V_{xc}[\rho]$. Note that in this language, the exact DFT appears as an approximation, which gives an approximate Green's function, and in which the exact self-energy is approximated by a static and local potential. The total energy is exact, but one would not learn this from the Luttinger-Ward formalism. Note also that the static approximation is a consequence of truncating the variable of interest, namely replacing full $G(\mathbf{r}, \tau, \mathbf{r}', \tau')$ by its diagonal components $\rho(\mathbf{r}) = \delta(\mathbf{r} - \mathbf{r}')\delta(\tau - \tau')G(\mathbf{r}\tau, \mathbf{r}'\tau')$.

In the Luttinger-Ward functional language, the DMFT appears as an approximation where the Green's function in the Φ functional is replaced by its local counterpart $G \to G_{local}$, and the Coulomb repulsion V_c by screened interaction $V_c \to U$, namely $\Phi^{DMFT} = \Phi_U[G_{local}]$. [5, 29] Note that the DMFT functional has exactly the same

form as the exact functional $\Phi_{Vc}[G]$, because all the skeleton Feynman diagrams constructed by G_{local} and U are summed up by DMFT [17], while in DFT the functional $E_{xc}[\rho]$ is unknown, and further approximation is necessary. The truncation of the variable of interest from G to G_{local} leads in DMFT to the self-energy, which is also local in space, but it keeps its dynamic nature. Other approximations such as Hartree-Fock or GW [18] can be similarly derived by replacing $\Phi_{Vc}[G]$ by some limited set of Feynman diagrams, i.e., truncation in space of Feynman diagrams, rather than truncation of the variable of interest.

There is some kind of disconnect between the DMFT functional $\Phi_U^{DMFT}[G_{local}]$, and the LDA functional $E_{xc}[\rho(\mathbf{r})]$, mostly because the auxiliary systems for the two methods are very different. The auxiliary system for LDA approximation is the uniform electron gas problem defined for continuum, in the absence of complexity of the solid. On the other hand, DMFT is usually associated with the lattice model like Hubbard model, where mapping to the local problem reduces to the Anderson impurity model, which does not have a unique continuum representation. The double-counting problem occurs because it is not clear what is the overlap between the two methods, i.e., what physical processes are accounted for in one and what in the other method.

It is useful to represent the DMFT method in the continuum $\mathbf{r}$ representation with the real space Projection/Embedding technique [9]. First we define the DMFT projector $\hat{P}$ such that it maps the Green's function, defined in the real space $G(\mathbf{r},\mathbf{r}')$, to the local Green's function also defined in the real space, i.e., $G_{local}(\mathbf{r},\mathbf{r}') = \hat{P}G(\mathbf{r},\mathbf{r}')$. Next we also write the screened Coulomb repulsion in the continuum space and we denote it by $V_{DMFT}(\mathbf{r},\mathbf{r}')$. The DMFT is then the method which sums all skeleton Feynman diagrams constructed by $G_{local}(\mathbf{r},\mathbf{r}')$ and $V_{DMFT}(\mathbf{r},\mathbf{r}')$, and hence the DMFT functional has exactly the same form as the exact functional, except that the variables V_c and G are replace by V_{DMFT} and G_{local}, respectively, i.e., $\Phi_{V_c}[G(\mathbf{r},\mathbf{r}')] \to \Phi_{V_{DMFT}}[G_{local}(\mathbf{r},\mathbf{r}')]$. [19] Note that this truncation of the Green's function $G(\mathbf{r},\mathbf{r}')$ to its local counterpart parallels the truncation of the Green's function to its diagonal component in theories that choose density as the essential variable, i.e., $\rho(\mathbf{r}) = G(\mathbf{r}\tau,\mathbf{r}'\tau')\delta(\mathbf{r}-\mathbf{r}')\delta(\tau-\tau')$.

More specifically, for the projector $\hat{P}$ we will use a set of quasi atomic orbitals, such that $G_{local}(\mathbf{r},\mathbf{r}') = \sum_{L,L'} \langle\mathbf{r}|\phi_L\rangle \langle\phi_L| G |\phi_{L'}\rangle \langle\phi_{L'}|\mathbf{r}'\rangle$ where $\langle\mathbf{r}|\phi_L\rangle = u_l(r)Y_L(\mathbf{r})$ are spheric harmonics times localized radial wave function. Note that locally the basis could be completed, in which case the DMFT becomes projector independent method, which depends only on the range of the projector. For the screened Coulomb repulsion, we will use Yukawa short-range interaction of the form $V_{DMFT}(\mathbf{r},\mathbf{r}') = \frac{e^{-\lambda|\mathbf{r}-\mathbf{r}'|}}{|\mathbf{r}-\mathbf{r}'|}$, but the precise form is arbitrary at this point.

After mapping the DMFT method to the continuous $(\mathbf{r},\mathbf{r}')$ Hilbert space, where DFT exchange-correlation is defined, it is easy to see what is the overlap between the two methods. The Hartree term is accounted for exactly in the LDA method, and has the form $E_{V_c}^H[\rho] = \frac{1}{2}\int d\mathbf{r}d\mathbf{r}'\rho(\mathbf{r})\rho(\mathbf{r}')V_c(\mathbf{r}-\mathbf{r}')$, while in DMFT it takes the following form $E^{H,DMFT} = \frac{1}{2}\int d\mathbf{r}d\mathbf{r}'(\hat{P}\rho(\mathbf{r}))(\hat{P}\rho(\mathbf{r}'))V_{DMFT}(\mathbf{r}-\mathbf{r}')$, which can also be written as $E^{H,DMFT} = E^H_{V_{DMFT}}[\hat{P}\rho]$, where $\hat{P}\rho = \delta(\mathbf{r}-\mathbf{r}')\delta(\tau-\tau')G_{local}(\mathbf{r}\tau,\mathbf{r}'\tau')$, and $E_{V_c}^H[\rho]$ is the exact Hartree functional defined above. The Hartree contribution to the DC within LDA+DMFT (or any other band structure method which includes the exact Hartree term) is thus $E^H_{V_{DMFT}}[\hat{P}\rho]$. This DC term thus corresponds to truncating the Green's function G and the Coulomb interaction V_c by their local/screened counterparts, i.e., $G \to \hat{P}G$ and $V_c \to V_{DMFT}$ in the functional.

For approximations, which truncate in the space of Feynman diagrams (such as Hartree-Fock or GW method), one can obtain the DMFT double-counting by applying both the truncation in space of Feynman diagrams as well as the DMFT truncation in variables of interest. [20] For the case of GW method, one can check diagram by diagram that the corresponding DMFT Feynman diagram is obtained by replacing G by $\hat{P}G$ and V_c by V_{DMFT} in each diagram, just like it was done above for the Hartree term. More precisely, the GW functional can be written as $\Phi^{GW}_{V_c}[G] = E^H_{V_c} - \frac{1}{2}\mathrm{Tr}\log(1 - V_c\, G\, G)$, where $G\,G = P$ is the convolution of two Green's functions (polarization function). The GW+DMFT double-counting is thus $E^{H,DMFT} - \frac{1}{2}\mathrm{Tr}\log(1 - V_{DMFT}\ (\hat{P}G)\,(\hat{P}G))$, which can be shortly written as $\Phi^{GW}_{V_{DMFT}}[\hat{P}G]$.

In the case of DFT+DMFT, the expansion in terms of Feynman diagrams does not exist, however, to identify the overlap between the two methods, this is not essential. Clearly, the double-counting in DFT+DMFT is obtained by the same procedure of replacing G by $\hat{P}G$ and V_c by V_{DMFT} in the DFT functional. This can be derived in two ways: i) first applying the DFT approximation to the exact functional ($\Phi \to E^H_{V_c} + E^{XC}_{V_c}$), followed by the DMFT approximation on the resulting functional ($G \to \hat{P}G$, $V_c \to V_{DMFT}$), or, ii) first applying the DMFT approximation ($\Phi \to \Phi_{V_{DMFT}}[\hat{P}G]$), followed by the DFT approximation on the resulting functional. In both cases, we arrive at

$$\Phi_{DC}^{DFT+DMFT} = E^H_{V_{DMFT}}[\hat{P}\rho] + E^{XC}_{V_{DMFT}}[\hat{P}\rho],$$

where Φ_{DC} is a functional of $\rho_{local} = \delta(\tau-\tau')\delta(\mathbf{r}-\mathbf{r}')\hat{P}G$ only, because DFT truncates the Green's function to its diagonal components. The explicit derivation for the exchange, and representative correlation term, is given in the supplementary information.

In LDA method, the exchange-correlation functional is obtained from the energy of the uniform electron gas. To

obtain the LDA+DMFT double-counting, one thus needs to solve the problem of the electron gas with the density that contains only "local" charge $\hat{P}\rho$, but where electrons interact with the screened V_{DMFT} interaction. [29]

Including the exact double-counting, the LDA+DMFT Φ functional is thus

$$\Phi^{LDA+DMFT}[G] = E^H_{V_c}[\rho] + E^{XC}_{V_c}[\rho] + \Phi_{V_{DMFT}}[\hat{P}G] - \\ -E^H_{V_{DMFT}}[\hat{P}\rho] - E^{XC}_{V_{DMFT}}[\hat{P}\rho], \quad (1)$$

where $\Phi_{V_{DMFT}}[\hat{P}G]$ is the DMFT functional which contains all Feynman diagrams constructed from $\hat{P}G$ and V_{DMFT}. This is the central equation of this paper, as it defines the LDA+DMFT approximation including the exact DC. The saddle point equations give the LDA+DMFT set of equations in the real space:

$$G^{-1} - G_0^{-1} = \hat{P}\frac{\delta\Phi_{V_{DMFT}}[G_{local}]}{\delta G_{local}} + \quad (2) \\ \left(\frac{\delta E^{HXC}_{V_c}[\rho]}{\delta\rho} - \hat{P}\frac{\delta E^{HXC}_{V_{DMFT}}[\rho_{local}]}{\delta\rho_{local}}\right)\delta(\mathbf{r}-\mathbf{r}')\delta(\tau-\tau')$$

where we used $E^{HXC}[\rho] \equiv E^H[\rho] + E^{XC}[\rho]$ and $\hat{P}G \equiv G_{local}$ [29].

The only difference between functional Eq. 1, and the usual LDA+DMFT implementation, is the presence of $E^{XC}_{V_{DMFT}}$. This is the semi-local exchange and LDA correlation functional of the electron gas interacting by the screened interaction, which we will in the following approximate by the Yukawa form, i.e., $V_{DMFT}(\mathbf{r},\mathbf{r}') = \frac{e^{-\lambda|\mathbf{r}-\mathbf{r}'|}}{|\mathbf{r}-\mathbf{r}'|}$. We will take here a constant λ, although generalization with space dependent $\lambda(\mathbf{r}-\mathbf{r}')$ is in principle possible. The semi-local exchange-density $\varepsilon^x_{V_{DMFT}}[\rho]$ (defined by $E^x[\rho] = \int d\mathbf{r}\rho(\mathbf{r})\varepsilon^x[\rho(\mathbf{r})]$), can be computed analytically, and takes the following form

$$\varepsilon^x_{V_{DMFT}}[\rho] = -\frac{C}{r_s}f(x)$$

where

$$f(x) = 1 - \frac{1}{6x^2} - \frac{4\arctan(2x)}{3x} + \frac{(12x^2+1)\log(1+4x^2)}{24x^4},$$

$C = \frac{3}{2}\left(\frac{9}{4\pi^2}\right)^{1/3}$, $r_s = \left(\frac{3}{4\pi\rho}\right)^{1/3}$, and $x = \left(\frac{9\pi}{4}\right)^{1/3}\frac{1}{\lambda r_s}$. The exchange potential $V^x = \frac{\delta}{\delta\rho}E^x[\rho]$ is then $V^x_{V_{DMFT}} = \frac{4}{3}\varepsilon^x_{V_{DMFT}} + \frac{1}{3}\frac{C}{r_s}x\frac{df}{dx}$.

The correlation part requires solution of the homogeneous electron gas problem interacting with Yukawa repulsion, which was solved by QMC [21–23]. Here we want to have an analytic expression for correlation energy at arbitrary λ and r_s. It is well established that G_0W_0 gives quite accurate correlation energy of the electron gas [24, 25], especially when computed from the Luttinger-Ward functional $\Gamma[G]$. We thus repeated G_0W_0 calculation for the electron gas, but here we use Yukawa interaction. We evaluate the total energy using the Luttinger-Ward functional of GW to achieve high accuracy. We then fit the correlation energy in the range of physically most relevant $r_s \in [0,10]$ and screenings $\lambda \in [0,3]$ (λ is measured in Bohr radius inverse) with the following functional form:

$$\varepsilon^c_{V^\lambda_c} = \frac{\varepsilon^c_{\lambda=0}}{1+\sum_{n=1}^4 a_n r_s^n} \quad (3)$$

The numeric values of a_n coefficients, obtained by the fit, are given in supplementary information.

Finally, the correlation potential is $V^c_{DMFT} = \frac{V^c_{\lambda=0}}{A(r_s,\lambda)} + \frac{\varepsilon^c_{\lambda=0}}{C(r_s,\lambda)}$, where $A(r_s,\lambda) = 1+\sum_{n=1}^4 a_n r_s^n$ and $C(r_s,\lambda) = 3[1+\sum_{n=1}^4 a_n r_s^n]^2/\sum_{n=1}^4 n\, a_n\, r_s^n$. Note that V^c should not be confused with V_c. The former is the correlation potential, and the latter is the Coulomb interaction. We take the unscreened correlation energy density $\varepsilon^c_{\lambda=0}$ (and unscreened potential) from the standard parametrization of the quantum Monte Carlo results, hence the G_0W_0 calculation is only used for renormalization of correlations by screening with Yukawa form.

Ce-α	n_f	V_{dc}/U
exact	0.997	0.424
nominal	1.002	0.500
FLL	1.035	0.533

TABLE I: LDA+DMFT valence and DC potential for α-Ce at $T = 200\,\mathrm{K}$. The local Coulomb repulsion in Ce is $U = 6\,\mathrm{eV}$.

In the following we present results for some of the most often studied correlated solids, namely, elemental Cerium, $SrVO_3$ and $LaVO_3$. We will use the symbol U for the value of the DMFT screened monopole interaction, as is customary in the literature. Note however, that the value of U gives a unique value of screening parameter λ needed in the exact DC [29]. Moreover, in Yukawa parametrization of interaction, U then also uniquely determines the other Slater integrals, such as the Hund's coupling [29].

We will use three different forms of DC functional: i) "exact", which we introduced above, ii) "FLL" stands for fully localized limit form introduced in Ref. 6, which has the simple form $V_{dc} = U(n-1/2) - J/2(n-1)$, and n stands for the correlated occupancy, c) and the "nominal" DC, introduced in Ref. 9, 10 and in Ref. 14 in the context of Hubbard-I approximation. The "nominal" V_{dc} takes the same form as "FLL" formula, but n in the formula is replaced by the nominal occupancy (n^0), i.e., corresponding to the nominal valence. We use LDA+DMFT implementation of Ref. 9.

The physical properties of correlated materials are very sensitive to the value of the local occupancy n_f,

SrVO3	n_{t2g+eg}	n_{t2g}	n_{eg}	V_{dc}^{t2g}/U	V_{dc}^{eg}/U
exact	2.223	1.507	0.716	1.384	1.406
nominal	2.251	1.541	0.710	1.443	1.444
FLL	2.529	1.699	0.830	1.943	1.943

TABLE II: LDA+DMFT results for $SrVO_3$ at $T = 200\,\mathrm{K}$ and $U = 10\,\mathrm{eV}$. Both $t2g$ and eg orbitals are treated by DMFT.

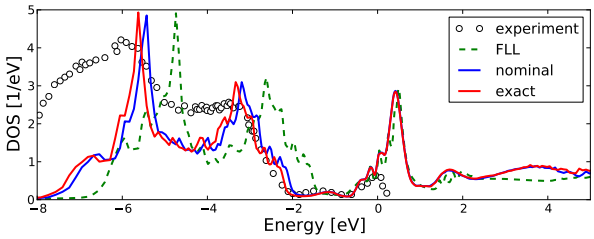

FIG. 1: (Color online) LDA+DMFT total density of states for $SrVO_3$ using three different DC potentials. Experimental photoemission is reproduced from Ref. 27. (parameters listed in table II).

and n_f is sensitive to the value of DC. In table I we show results for elemental Cerium in the α phase. All three DC functionals give very similar correlated occupancies n_f, and all are very close to nominal valence $n^0 = 1$. The actual value of the DC potential V_{dc} differs for less than $0.1\,U$, which leads to almost indistinguishable spectra on the real axis, and from the previously published results [9], hence we do not reproduce them here. We found a general trend in all materials studied that the exact DC is somewhat smaller then given by FLL formula. For Ce, the Hartree contribution to DC potential is $V_H = n_f U \approx 0.997\,U$, the semi-local exchange contribution is $V_x \approx -0.485\,U$ and LDA correlation is $V_c \approx -0.088\,U$, hence the total DC potential is $V_H + V_x + V_c \approx 0.424U$, which is slightly smaller than FLL formula $U(n_f - 1/2) - J/2(n_f - 1) \approx 0.533U$ or nominal formula $U(n_f^0 - 1/2) - J/2(n_f^0 - 1) = 0.5U$. It is interesting to note that the semi-local exchange used in LDA is quite different from the exact exchange value. The latter is only $|V_F| = Un/14 \approx 0.071\,U$, a substantially smaller value then the semi-local exchange $|V_x| \approx 0.485\,U$. This shows why DC within LDA+DMFT is so different from the Hartree-Fock value of the DMFT self-energy, i.e., $\Sigma(\omega = \infty)$.

Next we present tests for $SrVO_3$, which is a metallic transition metal oxide with nominally single electron in the t2g shell. Near the Fermi level E_F, there are mostly $t2g$ states. The majority of eg states are above E_F, however, due to strong hybridization with oxygen some part of eg orbitals also gets filled. There are two ways the DMFT method can be used here. In the first case, one can treat only the $t2g$ shell within DMFT. The vast majority of DMFT calculations for SrVO3 were done in this way. In this case, all three DC potentials again give very similar results and the spectra is almost indistinguishable from previously published results in Ref. 10. One can also treat dynamically with DMFT the entire d shell. This case is presented in Table II and spectra in Fig. 1. One can notice that the exact and the nominal DC give very similar n_d, while the FLL formula gives 14% larger n_d. This is because the value of the DC potential is substantially larger ($\approx 40\,\%$) when using FLL as compared to exact case. It is nevertheless comforting to see that 40% error in double-counting still does not leads to major failure of LDA+DMFT. We plot the spectra in Fig. 1, to show how this change in V_{dc} leads to shift of oxygen-p spectra relative to vanadium-d states. For the exact DC, the oxygen peak positions match very well with the experimentally measured spectra. The nominal valence is quite close to the exact spectra, while FLL formula leads to an upward shift of oxygen for roughly 0.6 eV, which is still relatively small compared to the difference in the double-counting potentials, which is $V_{dc}^{FLL} - V_{dc}^{exact} \approx 5.37\,\mathrm{eV}$.

LaVO3(t2g-only)	n_{t2g}	V_{dc}^{a1g}/U	$V_{dc}^{eg'}/U$
exact	2.014	1.195	1.193
nominal	2.074	1.450	1.450
FLL	2.099	1.544	1.544

TABLE III: LDA+DMFT results for $LaVO_3$ at $T = 200\,\mathrm{K}$ and $U = 10\,\mathrm{eV}$. Only $t2g$ orbitals are treated by DMFT.

LaVO3(t2g+eg)	n_{t2g+eg}	n_{t2g}	n_{eg}	V_{dc}^{a1g}/U	$V_{dc}^{eg'}/U$	V_{dc}^{eg}
exact	2.444	2.048	0.397	1.596	1.599	1.665
nominal	2.344	2.032	0.312	1.458	1.458	1.458
FLL	2.706	2.167	0.540	2.114	2.114	2.114

TABLE IV: LDA+DMFT results for $LaVO_3$ at $T = 200\,\mathrm{K}$ and $U = 10\,\mathrm{eV}$. Both $t2g$ and eg orbitals are treated by DMFT.

Next we present results for the Mott insulating oxide $LaVO_3$, which is solved in two ways, i) treating only the $t2g$ orbitals dynamically with DMFT, presented in Table III and Fig. 2a, and ii) treating both $t2g$ and eg with DMFT. In the first case, the valences are similar in all three double-counting formulas. The $t2g$ occupancy is very close to nominal value of 2. The exact double-counting is again smaller than given by FLL or nominal formula, which leads to a slightly larger splitting between oxygen-p and V-d states, i.e., slight upward shift of oxygen states in Fig. 2a. In case ii) displayed in Fig. 2b and tabulated in table IV, where both the $t2g$ and eg orbitals are treated by DMFT, the FLL formula dramatically fails, as it overestimates the valence, i.e., $n_d^{FLL} - n_d^{exact} \approx 0.26$. While the Mott gap does not entirely collapse, it is severely underestimated by FLL

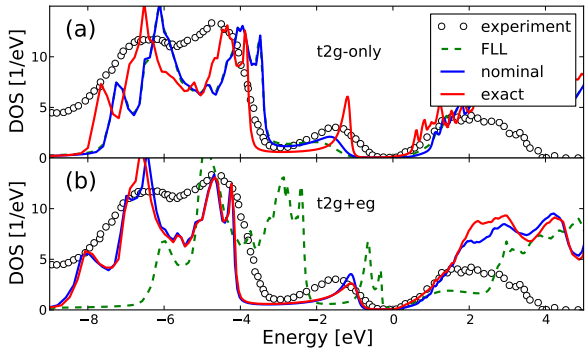

FIG. 2: (Color online) LDA+DMFT total density of states for $LaVO_3$ using the three different DC formulas. (a) only $t2g$ orbitals are treated by DMFT (b) both $t2g$ and eg orbitals are treated dynamically. Experimental photoemission is reproduced from Ref. 28.

formula. The nominal valence, however, gives very similar results as the exact DC. This improvement of nominal DC as compared to FLL was pointed our in Refs. 9, 10, and was found to hold not just in transition metal oxides but also in actinides [26]. The $t2g$ occupancy n_{t2g} in the nominal and exact DC is very close to nominal value of 2, equal to the scheme i) presented above. It is therefore not surprising that the spectra in Fig. 2a, and Fig. 2b are similar, with slight improvement compared to experiment when eg orbitals are also treated by DMFT.

In summary, we presented continuum representation of the Dynamical Mean Field Theory, which allowed us to derive an exact double-counting between Dynamical Mean Field Theory and Density Functional Theory. The implementation of exact double-counting for solids shows the improved agreement with experiment as compared to standard FLL formula. Previously introduced nominal DC formula [9, 10] is in very good agreement with exact double-counting derived here.

This work was supported Simons foundation under project "Many Electron Problem", and by NSF-DMR 1405303.

[1] P. Hohenberg, and W. Kohn, Phys. Rev. **136**, B864 (1964).
[2] A. Georges, and G. Kotliar, Phys. Rev. B **45**, 6479 (1992).
[3] A. Georges, G. Kotliar, W. Krauth, and M. J. Rozenberg, Rev. Mod. Phys.**68**, 13 (1996).
[4] Anisimov, Poteryaev, Korotin, Anokhin, Kotliar J. Phys.: Condens. Matter 9, 7359 (1997); Lichtenstein, Katsnelson Phys. Rev. B 57, 6884 (1998).
[5] For a review see: G. Kotliar, S. Y. Savrasov, K. Haule, V. S. Oudovenko, O. Parcollet, and C. A. Marianetti, Rev. Mod. Phys. **78**, 865 (2006).
[6] M. T. Czyzyk, and G. A. Sawatzky, Phys. Rev. B **49** 14211 (1994).
[7] V. I. Anisimov, F. Aryasetiawan, and A. I. Lichtenstein, J. Phys.: Condens. Matter **9**, 767 (1997).
[8] M. Karolak, G. Ulm, T. Wehling, V. Mazurenko, A. Poteryaev, A. Lichtenstein, Journal of Electron Spectroscopy and Related Phenomena **181** 11 (2010).
[9] K. Haule, C.-H. Yee, and K. Kim, *Phys. Rev. B* **81**, 195107 (2010).
[10] K. Haule, T. Birol, and G. Kotliar, Phys. Rev. B **90**, 075136 (2014).
[11] H. Park, A. J. Millis, and C. A. Marianetti, Phys. Rev. B **89**, 245133 (2014).
[12] A. van Roekeghem, T. Ayral, J. M. Tomczak, M. Casula, N. Xu, H. Ding, M. Ferrero, O. Parcollet, H. Jiang, S. Biermann, Phys. Rev. Lett **113**, 266403 (2014).
[13] Juho Lee and Kristjan Haule, Phys. Rev. B **91**, 155144 (2015).
[14] L.V. Pourovskii, B. Amadon, S. Biermann, and A. Georges, Phys. Rev. B **76**, 235101 (2007).
[15] J. M. Luttinger, and J. C. Ward, Phys. Rev. **118**, 1417 (1960).
[16] G. Baym and L. P. Kadanoff, Phys. Rev. **124**, 287 (1961).
[17] L. Pollet, N. V. Prokofev, and B. V. Svistunov, Phys. Rev. B **83**, 161103(R) (2011).
[18] L. Hedin, Phys. Rev. **139**, A796 (1965).
[19] R. Chitra and G. Kotliar, Phys. Rev. B **62**, 12715 (2000).
[20] S. Biermann, F. Aryasetiawan, and A. Georges, Phys. Rev. Lett **90**, 086402 (2003).
[21] D. Ceperley, G. V. Chester, and M. H. Kalos, Phys. Rev. B **16**, 3081 (1977).
[22] D. M. Ceperley and B. J. Alder, Phys. Rev. Lett **45**, 566 (1980).
[23] M. A. Ortiz, and R. M. Mendez-Moreno, Phys. Rev. A **36**, 888 (1987).
[24] P. Garcia-Gonzalez and R. W. Godby, Phys. Rev. B **63**, 075112 (2001).
[25] B. Holm and U. von Barth Phys. Rev. B **57**, 2108 (1998).
[26] J. H. Shim, K. Haule and G. Kotliar, Eur. Phys. Lett. **85**, 17007 (2009).
[27] K. Yoshimatsu, T. Okabe, H. Kumigashira, S. Okamoto, S. Aizaki, A. Fujimori, and M. Oshima, Phys. Rev. Lett. **104** 147601 (2010).
[28] K. Maiti and D. D. Sarma, Phys. Rev. B **61**, 2525 (2000).
[29] For more information, see supplementary information.